

QW115 Fig. 3. Polarization of reflection-SHG beam vs. pump polarization for different incident angles.

pulse energy is the highest. On the other hand, when the pump polarization is vertical, the SHG pulse energy is the lowest. For the first time, we have also measured the SHG polarization vs. the pump polarization (Fig. 3). For an incident angle of $\theta = 23^\circ$ for the pump beam, when its polarization angle is around 52° , the SHG polarization is vertical. However, when the pump polarization is horizontal or vertical, the SHG polarization is horizontal. On the other hand, for $\theta = 60^\circ$ the SHG polarization is always more or less horizontal (i.e. the polarization angle is $\pm 5^\circ$).

These structures have potential applications in difference-frequency generation and optical parametric amplification for generating and amplifying mid-IR beams (e.g. $980 \text{ nm} + 1.55 \text{ }\mu\text{m} \Rightarrow 2.66 \text{ }\mu\text{m}$ while amplifying $1.55 \text{ }\mu\text{m}$). Reflection-SHG may be eventually developed to a technique for measuring indices of refraction above band-gaps. It can also be used to probe layer thickness and element concentration during the MBE growth of multilayers.

*Univ. of Arkansas, USA

**NRL, USA

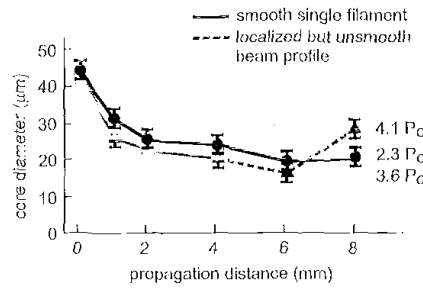
1. R. Normand, R.L. Williams, F. Chatenoud, Electron. Lett. **26**, 2088 (1990).
2. Y.J. Ding, J.B. Khurgin, S.J. Lee, Phys. Rev. Lett. **75**, 429 (1995).
3. J.P. van der Ziel and M. Ilegems, Appl. Phys. Lett. **28**, 437 (1976).
4. S. Janz, C. Fernando, H. Dai, F. Chatenoud, M. Dion, R. Normandin, Opt. Lett. **18**, 589 (1993).
5. Y.J. Ding and J.B. Khurgin, J. Opt. Soc. Am. B **14**, 2161 (1997).

QW116

Uncollapsed self-focusing of femtosecond pulses in dielectric media due to the saturation of nonlinear refractive index

Tai-Wei Yau, Chau-Hwang Lee,^{*} Jyhpyng Wang,^{**} Institute of Electro-Optical Engineering, National Taiwan Univ., P.O. Box 23-166, Taipei 106, Taiwan; E-mail: jwang@tl.iam.s.sinica.edu.tw

Single-filament propagation of self-focused femtosecond pulses in dielectric media has



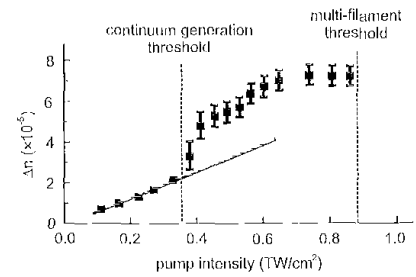
QW116 Fig. 1. Beam-diameter evolution in sapphire. For high-power pulses propagating longer than 4 mm, the beam profiles become less smooth, therefore beam diameter is less well-defined (dashed parts).

been observed and applied to stable white-light continuum generation.¹ The observation is contradictory to early computer simulation, where beam collapse was predicted.² In many recent numerical models, effects that could balance self-focusing, such as non-paraxiality, multiphoton ionization, group-velocity dispersion, etc., have been studied to show the possibility of uncollapsed self-focusing of femtosecond pulses. Nevertheless, systematic measurements are needed to construct a clear picture of the propagation of femtosecond pulses under extreme self-focusing.

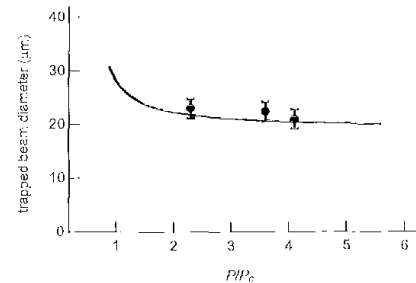
In this work we analyze the spatiotemporal waveform evolution of self-focused high-power femtosecond pulses with a three-dimensional phase-retrieval cross-correlation technique.³ Figure 1 shows the FWHM beam diameter evolution for 810-nm, 270-fs pulses propagating in sapphire due to self-focusing. Within the experimental power range (2.3–4.1 P_c), the beams shrink to a diameter of 20–25 μm in 4-mm propagation, and no catastrophic beam collapse was observed. Within the parameter space of our previous dye-laser experiments⁴ and these experiments, this uniform self-focused beam size appears to be insensitive to the initial beam size, power, and wavelength.

In search of the mechanism that blocks runaway self-focusing, we studied the intensity dependence of the refractive index with a cross-polarization modulation experiment. We measured the polarization rotation of a test beam induced by a high-power pump beam all the way to the threshold of multi-filament propagation. From the polarization rotation angle we deduce the change in refractive index Δn . Figure 2 shows the induced Δn as a function of pump intensity. When the pump intensity is below the point where white-light continuum emerges, Δn is proportional to the pump intensity I : $\Delta n = n_2 I$. The measured n_2 in Fig. 2 is $2.4 \times 10^{-16} \text{ cm}^2/\text{W}$, close to the data ($2.5 \times 10^{-16} \text{ cm}^2/\text{W}$ for sapphire) in Ref. 5. When I is increased to $4 \times 10^{11} \text{ W/cm}^2$, white-light continuum starts to become detectable. At the same time, Δn increases rapidly with intensity. Finally Δn saturates to $\Delta n_{\text{max}} \approx 7 \times 10^{-5}$.

The saturation of n_2 explains uncollapsed self-focusing. Under the aberrationless approximation, we model the self-focused beam



QW116 Fig. 2. The intensity-dependent change of refractive index.



QW116 Fig. 3. FWHM diameters of the self-trapped beams calculated by the graded-index waveguide model.

as a cylindrical waveguide with a parabolic refractive-index profile:

$$n(r) = \begin{cases} n_c [1 - \alpha (r/a)^2]^{1/2} & r < a \\ n_0 & r \geq a \end{cases} \quad (1)$$

where n_0 is the linear refractive index, n_c is the refractive index at the beam center, and $\alpha = 1 - (n_0/n_c)^2$. Following the analysis in Ref. 6, the minimum radius a of this cylindrical waveguide for the propagation of the fundamental transverse mode is

$$a = \frac{2}{k_0 \sqrt{n_c^2 - n_0^2}} \quad (2)$$

where k_0 is the wave number in free space. If self-focusing shrinks the beam radius to a with n_c satisfying Eq. (2), the self-consistent condition of the “waveguide” is met. This criterion has been used to calculate the size of a self-induced optical fiber with a step refractive-index profile in an idealized saturation medium.⁷ We use this graded-index self-consistent waveguide model and the saturated Δn in Fig. 2 to calculate the trapped beam diameter as a function of power. As shown in Fig. 3, the result is in good agreement with experiments.

The beam-diameter evolution measurement and the intensity-dependent refractive index measurement above thus together point out that in sapphire, single-filament beam trapping is a result of n_2 saturation.

*Inst. of Atomic and Molecular Sciences, Taiwan

**Also with Inst. of Atomic and Molecular Sciences and Department of Engineering Natl. Taiwan Univ., Taiwan

1. M.K. Reed, M.K. Steiner-Shepard, D.K. Negus, “Widely tunable femtosecond optical parametric amplifier at 250 kHz with

- a Ti:sapphire regenerative amplifier," *Opt. Lett.* **19**, 1855–1857 (1994).
- P.L. Kelley, "Self-focusing of optical beams," *Phys. Rev. Lett.* **15**, 1005–1008 (1965).
 - T.-W. Yau, C.-H. Lee, J. Wang, "Spatial-temporal field distribution of self-focused femtosecond pulses," *Ultrafast Phenomena XI*, T. Elsaesser, J.G. Fujimoto, D.A. Wiersma, W. Zinth, eds., (Springer, Berlin, 1998), pp. 106–108.
 - Y.-Y. Hwang, Y.-H. Kuo, C.-H. Lee, J. Wang, in *Conference on Lasers and Electro-Optics*, Vol. 11 of 1997 OSA Technical Digest Series (Optical Society of America, Washington, D.C., 1997), paper CTuP22.
 - M.J. Weber, D. Milam, W.L. Smith, "Non-linear refractive index of glasses and crystals," *Opt. Eng.* **17**, 463–469 (1978).
 - A. Yariv, *Optical Electronics*, 4th ed. (Saunders College Publishing, Philadelphia, 1991), Sec. 3.4.
 - A.W. Snyder, D.J. Mitchell, L. Poladian, F. Ladouceur, "Self-induced optical fibers: spatial solitary waves," *Opt. Lett.* **16**, 21–23 (1991).

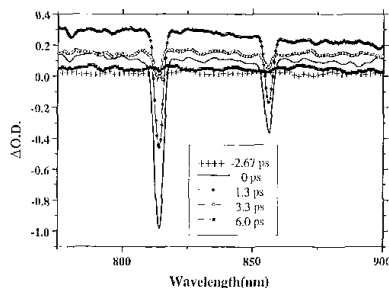
QW117

Raman gain saturation, pump depletion and two-photon absorption in pTS

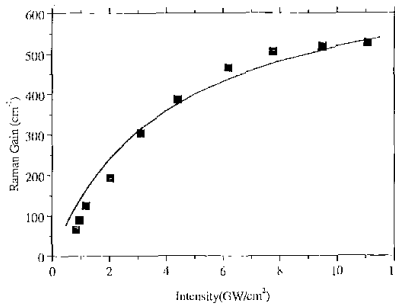
Steven R. Flom, J.R. Lindle, F.J. Bartoli, Mingguo Liu,* George I. Stegeman,* *Optical Sciences Division, NRL, Washington, DC 20375, USA; E-mail: flom@nrl.navy.mil*

Single crystals of the polydiacetylene, poly[2,4-hexadiyne-1,6-diol-bis(p-toluenesulfonate)] (pTS) have been studied in the near resonant regime by transient absorption spectroscopy. Figure 1 shows the changes observed in the absorption spectra at short times surrounding the arrival of the 726-nm laser pulse. The experiment is performed by monitoring the transmission of a continuum probe in the presence of a ~1-ps high intensity pump pulse. The prominent negative going peaks are due to stimulated Raman scattering arising from the carbon-carbon double and triple bonds along the polymer backbone. The broad induced absorption is the result of population of an excited state produced through two-photon excitation.

The pump intensity dependence of the first Raman peak has been measured at zero time



QW117 Fig. 1. Transient absorption spectra of a 57- μm -thick single crystal of pTS. The excitation wavelength is 726 nm and the intensity is 5.5 GW/cm^2 .



QW117 Fig. 2. The squares are the observed data points while the solid line is a fit to the data.

delay and is shown in Fig. 2. The solid line in the figure is a result of fitting the data to a model for Raman gain in a strong two-photon absorbing medium, described below.

Simple modeling of the stimulated Raman gain coefficient¹ predicts that the small signal gain should depend linearly on the pump intensity. Clearly the data deviates from linear behavior for the measurement range. Successful modeling of the observed gain saturation is accomplished by taking into account pump intensity attenuation due to two-photon absorption. In addition, the two-photon induced population absorbs light at the Stokes wavelength. A value of 340 cm^2/GW , measured independently by both nonlinear transmission² and z-scan³ experiments, was used for the two-photon absorption coefficient. The full model takes into account the gaussian spatial and temporal profiles of both the pump and the probe and yields an intensity dependent gain coefficient of 600 cm^2/GW in the presence of two-photon absorption.

The system of equations used in the model are:

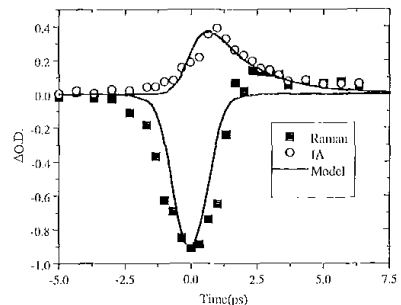
$$\frac{dI}{dz} = -\alpha I - \alpha_2 I^2$$

$$\frac{dN}{dt} = \frac{\alpha_2}{2\hbar\omega} I^2$$

$$\frac{dS}{dz} = gIS - \alpha_S S - \sigma_S NS$$

where I is the pump intensity, α is the linear absorption coefficient, α_2 is the two-photon absorption coefficient, S is the intensity of the continuum probe at the Raman wavelength, g is the Raman gain, α_S and σ_S are the ground state linear absorption coefficient and excited state absorption cross section at the Raman wavelength. While these equations can be solved analytically if σ_S is sufficiently small, Fig. 1 shows that this is not the case. The fit in Fig. 2 is the result of numerical integration of the equations using only g as an adjustable parameter. The observed saturation in the data is largely attributable to depletion of the pump through two-photon absorption.

The data in Fig. 1 show that the maximum of the Raman signal precedes that of the induced absorption. Figure 3 shows the time dependence of the two spectral regions along with a calculation based on the model described above. Both the data and the model



QW117 Fig. 3. Time dependence of the induced absorption (IA) and Raman signal.

show the delayed appearance of the induced absorption. The two-photon produced population continues to grow after the maximum of the pump laser pulse and decays with the characteristic lifetime⁴ of the lowest excited state of pTS. The Raman pulse essentially follows the time dependence of a cross correlation of the pump and probe pulse though there is subtle evidence of pulse shaping due to the excited state population.

The stimulated gain coefficient extracted from the data exceeds that of commonly used gain media¹ by at least an order of magnitude. Even in the presence of significant pump depletion through strong two-photon absorption and excited state absorption, raw gains of almost an order of magnitude are observed (see Fig. 1). Taken together these data suggest that this class of polymers may have promise for Raman laser and differential amplification applications, particularly at longer wavelengths where the two-photon absorption coefficient is small.

*CREOL, USA

- Y.R. Shen, *The Principles Of Nonlinear Optics* (Wiley Interscience, New York, 1984) Chap. 10.
- S.R. Flom, J.R. Lindle, F.J. Bartoli, M. Liu, G.I. Stegeman, "Nonlinear Optical Response of pTS Near the Band Edges," in *Organic Thin Films for Photonics Applications*, OSA Technical Digest (Optical Society of America, Washington DC, 1999), pp. 214–216.
- B. Lawrence, W.J. Torruellas, M. Cha, M.L. Sundheimer, G.I. Stegeman, J. Meth, S. Etemad, G. Baker, "Identification and Role of Two-Photon Excited States in a π -Conjugated Polymer," *Phys. Rev. Lett.* **73**, 597 (1994); H. Shim, M. Liu, C. Hwangbo, G.I. Stegeman, "Four-Photon Absorption in the Single-Crystal Polymer bis(paratoluene) Sulfonate," *Opt. Lett.* **23**, 430 (1998).
- B.I. Greene, J. Orenstein, R.R. Millard, L.R. Williams, "Picosecond Relaxation Dynamics in Polydiacetylene-pTS," *Chem. Phys. Lett.* **139**, 381 (1987); B.I. Greene, J.F. Mueller, J. Orenstein, D.H. Rapkine, S. Schnitt-Rink, M. Thackur, "Phonon Mediated Optical Nonlinearity in Polydiacetylene," *Phys. Rev. Lett.* **61**, 325 (1988).